

# UC Irvine

## UC Irvine Previously Published Works

### Title

The Canopy Horizontal Array Turbulence Study

### Permalink

<https://escholarship.org/uc/item/70g5k7xx>

### Journal

Bulletin of the American Meteorological Society, 92(5)

### ISSN

0003-0007

### Authors

Patton, Edward G

Horst, Thomas W

Sullivan, Peter P

et al.

### Publication Date

2011-05-01

### DOI

10.1175/2010bams2614.1

### Copyright Information

This work is made available under the terms of a Creative Commons Attribution License, available at <https://creativecommons.org/licenses/by/4.0/>

Peer reviewed

# THE CANOPY HORIZONTAL ARRAY TURBULENCE STUDY

BY EDWARD G. PATTON, THOMAS W. HORST, PETER P. SULLIVAN, DONALD H. LENSCHOW, STEVEN P. ONCLEY, WILLIAM O. J. BROWN, SEAN P. BURNS, ALEX B. GUENTHER, ANDREAS HELD, THOMAS KARL, SHANE D. MAYOR, LUCIANA V. RIZZO, SCOTT M. SPULER, JIELUN SUN, ANDREW A. TURNIPSEED, EUGENE J. ALLWINE, STEVEN L. EDBURG, BRIAN K. LAMB, RONI AVISSAR, RONALD J. CALHOUN, JAN KLEISSL, WILLIAM J. MASSMAN, KYAW THA PAW U, AND JEFFREY C. WEIL

Observations from a California walnut orchard—before and after leaves emerged—should help advance understanding, simulation capabilities, and modeling of coupled vegetation–atmosphere–land surface interactions.

**MOTIVATION.** Vegetation covers nearly 30% of Earth’s land surface and influences climate through the exchanges of energy, water, carbon dioxide, and other chemical species with the atmosphere (Bonan 2008). The Earth’s vegetation plays a critical role in the hydrological, carbon, and nitrogen cycles and also provides habitat and shelter for biota that deliver essential ecosystem services, such as pollination. In addition, living foliage produces a variety of chemical compounds that can significantly influence the oxidation capacity (cleansing ability) of the atmosphere (e.g., Fuentes et al. 2000; Guenther et al. 2006) and global aerosol distributions (e.g., Hallquist et al. 2009). Plant–atmosphere interactions can also have negative effects with billions of dollars each year lost from wind damage to forests and crops. Therefore, understanding the processes controlling vegetation–atmosphere exchange at the most fundamental level is of critical importance for weather, climate, and environmental forecasting as well as for agricultural and natural resource management.

*Turbulent exchange within and above vegetation.* Turbulence in plant canopies is unique from turbulence elsewhere in the planetary boundary layer (PBL), in that the majority of the atmosphere’s momentum is

absorbed throughout the canopy depth as drag on the plant elements rather than as friction on the ground. Over the years, it has become clear that the bulk of the exchange between the canopy layers and aloft occurs through turbulent eddies that are of similar scale to the canopy itself rather than to the scale of the individual canopy elements (e.g., Gao et al. 1989). Recent studies postulate that these eddies are produced by larger PBL-scale turbulent motions triggering an instability associated with the inflection in the velocity profile induced by plant canopy drag (e.g., Raupach et al. 1996; Finnigan et al. 2009).

The ground and vegetation can act as both scalar sources and sinks. Within the soil, heterotrophic and autotrophic respiration is a source of CO<sub>2</sub> throughout the year that varies seasonally with soil temperature and moisture (e.g., Ryan and Law 2005), while decomposing litter and soil microbes can produce volatile organic compounds (VOCs) (e.g., Leff and Fierer 2008). The distribution of canopy sources/sinks depends on the amount and state of the canopy foliage, which varies throughout the seasonal cycle for deciduous trees: from bare limbs in winter (no photosynthesis and an open canopy) to rapid growth in spring (increasing photosynthesis and canopy density) to maturity in summer (more constant

photosynthesis and canopy density) to senescence and leafdrop in fall (decreasing photosynthesis and canopy density). Thus, a broad spectrum of different conditions occurs through the year, and dynamical and scalar fluxes exhibit height dependence and seasonal variability. State-of-the-art analytic or closure models describing these processes are only beginning to address these complexities (e.g., Harman and Finnigan 2008).

**Linking models and measurements.** Large-eddy simulation (LES) is one of the best available numerical tools capable of linking turbulent motions over scales ranging from the microscale to the mesoscale (e.g., Wyngaard 1984). Using a three-dimensional grid, LES solves the time-dependent filtered Navier–Stokes equations to simulate all resolved scales of motion as they evolve in space and time while using a subfilter-scale (SFS) model to parameterize only the smallest scales (Pope 2000). Another important component of LES is that active, passive, and reactive scalars can be incorporated. As numerical techniques and computational capabilities have improved over the last 30 years, LES results have become a key complement to measurements.

In canopy-resolving LES,<sup>1</sup> the pressure and viscous drag associated with the vegetation elements serve as an important momentum sink, which induces an inflection in the velocity profile and introduces turbulent length scales such as the canopy depth or the eddy penetration depth (e.g., Finnigan et al. 2009). Intriguingly, increased grid resolution improves the accuracy of the simulation by better resolving the velocity gradient at canopy top; contrast this with LES over unresolved roughness where increased resolution continually reduces the scale of the peak in the vertical velocity energy spectrum, which forces continued reliance on SFS parameterizations (Sullivan et al. 2003).

**Previous HATS campaigns.** Despite its myriad contributions to understanding turbulent flows, LES does have shortcomings and needs to be validated and improved to deal with complex flows, especially for surface layers where dependence on the SFS model increases. To address this issue, the National Center for Atmospheric Research (NCAR) in collaboration with several university groups recently carried out two pioneering observational studies to improve subfilter-scale parameterizations over flat terrain with sparse low-lying vegetation [Horizontal Array Turbulence Study (HATS)] and over the ocean [Ocean HATS (OHATS)] (e.g., Sullivan et al. 2003; Horst et al. 2004). These studies applied a technique first proposed by Tong et al. (1998) that uses horizontal arrays of 14–18 sonic anemometers/thermometers deployed at two levels to measure spatially filtered variables and their gradients. These datasets provide an observational basis for validating and developing SFS closure approximations.

**Canopy influence on SFS motions.** Vegetation adds complexity to SFS motions. Canopy elements are nonuniformly distributed spatially (often occurring in clumps) and thereby spread sources/sinks of momentum and scalars throughout the canopy layer. For example, large-scale turbulence interacting with clumped elements can rapidly break down into smaller wake-scale motions, thereby short-circuiting the inertial energy cascade (Finnigan 2000). In addition, depending on the density of the canopy elements, the spatially distributed plant structures intercept (and are heated by) solar radiation during

**AFFILIATIONS:** PATTON, HORST, SULLIVAN, LENSCHOW, ONCLEY, BROWN, BURNS, GUENTHER, HELD,\* KARL, MAYOR,\* RIZZO,\* SPULER, SUN, AND TURNIPSEED—National Center for Atmospheric Research,\* Boulder, Colorado; ALLWINE, EDBURG,\* AND LAMB—Washington State University, Pullman, Washington; AVISSAR\*—Duke University, Durham, North Carolina; CALHOUN—Arizona State University, Tempe, Arizona; KLEISSL—University of California, San Diego, La Jolla, California; MASSMAN—USDA Forest Service, Fort Collins, Colorado; PAW U—University of California, Davis, Davis, California; WEIL—University of Colorado, Boulder, Colorado

\***CURRENT AFFILIATIONS:** HELD—University of Bayreuth, Bayreuth, Germany; MAYOR—California State University, Chico, California; RIZZO—University of Sao Paulo, Sao Paulo, Brazil; EDBURG—University of Idaho, Moscow, Idaho; AVISSAR—University of Miami, Miami, Florida

\*The National Center for Atmospheric Research is sponsored by the National Science Foundation.

**CORRESPONDING AUTHOR:** Edward Patton, National Center for Atmospheric Research, P.O. Box 3000, Boulder, CO, 80307–3000  
E-mail: patton@ucar.edu

The abstract for this article can be found in this issue, following the table of contents.

DOI:10.1175/2010BAMS2614.1

In final form 15 October 2010  
©2011 American Meteorological Society

<sup>1</sup> Canopy-resolving LES means that the equations of motion are spatially filtered in the presence of solid canopy elements, which generates terms in the equations accounting for the canopy-induced pressure and viscous drag on the fluid.

daytime and radiatively cool faster than a bare surface at night. As a result, in daytime (nighttime) the leaves can create stable (unstable) conditions within the canopy when the overlying atmosphere is unstably (stably) stratified. Given the fundamentally different mechanisms of momentum and heat transport to and from the foliage (where momentum transport occurs largely through pressure drag and heat transport occurs through the much slower process of molecular diffusion), within-canopy turbulence can also completely collapse and decouple from the above-canopy turbulence (Belcher et al. 2008).

The majority of current SFS parameterizations used in canopy LES assume that the unresolved SFS motions fall within the inertial subrange and that all wake-scale motions immediately dissipate to heat (e.g., Shaw and Schumann 1992). Recently, Shaw and Patton (2003) attempted to improve SFS parameterizations for canopy-resolving LES by allowing wake-scale motions to transport turbulence; however, in this study, the inertial range assumptions were still required. Finnigan (2000) modified Kolmogorov's energy cascade concept to include pressure and viscous drag effects of plants, but this theory has not been thoroughly tested. At this point, the character of within-canopy small-scale motions, the role played by eddies shed in the lee of the plant elements, and how these wake-scale motions affect scalar and momentum transport are largely unknown. We speculate that spatial variations of the canopy elements modify SFS motions through canopy-induced stratification and scalar/momentum source/sink distributions.

When the Canopy Horizontal Array Turbulence Study (CHATS) experiment was originally proposed, observing SFS variables within the canopy had not been previously attempted. Recently, however, Zhu et al. (2007) reported an attempt to measure SFS momentum fluxes in a wind tunnel model canopy using laser Doppler velocimetry. Their results support the importance of canopy influences

on SFS motions but lack the ability to assess the impact of vegetation on scalar transport and to characterize the impact of the larger scales of motion and thermal stratification in the planetary boundary layer.

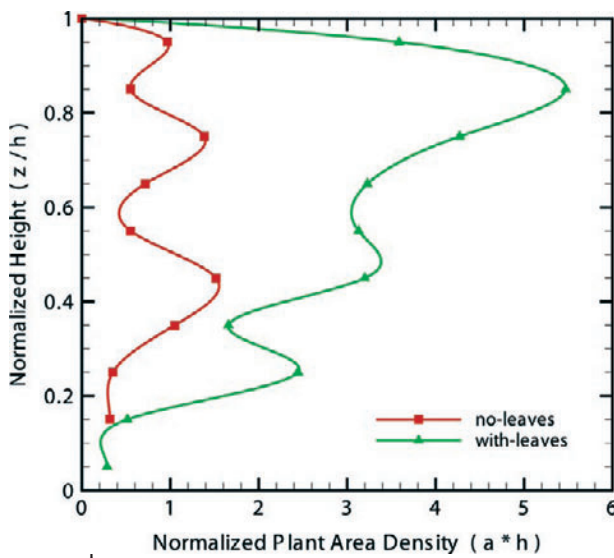
*Hence, CHATS.* In practice, most canopy measurements are typically limited to time averages from vertical arrays of sensors at a single location. Exceptions to this have become more common in recent years, with explicit spatial averaging in wind tunnel model canopies (e.g., Böhm et al. 2000) and multiple tower arrays in the field focused on horizontal transport (e.g., Feigenwinter et al. 2008). Through the use of a wide range of remote and in situ sensing systems using novel deployment strategies, the CHATS campaign aspires to obtain a dataset capable of uncovering the links between canopy sources/sinks of momentum and scalars and the spatial structure of canopy turbulence with an emphasis on improving the fidelity of canopy-resolving LES and its ability to realistically reproduce scalar and momentum transport within and above vegetated surfaces. Through both the observations themselves and improved canopy LES, the CHATS dataset sets up a framework to test, evaluate, and refine unified one-dimensional column models of coupled land surface–atmosphere



**FIG. 1.** Images from Google Earth depicting the location of Cilker Orchards. Upper left image shows the location of the orchard with respect to Vacaville and Davis, CA. Bottom right image shows the location of the various instrumentation with respect to Cilker Orchards. The yellow square depicts the 800 m × 800 m Cilker property of central focus, which sits in the northwest quadrant of the larger orchard block.



**FIG. 2.** Photos showing the orchard (top) before and (bottom) after leafout.



of the orchard is about 21 m above sea level. United States Department of Agriculture survey maps classify the majority of the soil in the block as Yolo silty clay loam with small portions of Yolo loam and Brentwood clay loam (<http://websoilsurvey.nrcs.usda.gov/app/WebSoilSurvey.aspx>).

Twenty-four years of data from the California Irrigation Management Information System (CIMIS; <http://wwwcimis.water.ca.gov>) in Davis show the

**FIG. 3.** PAD profiles measured during CHATS. These profiles are averaged over measurements taken throughout each month of intensive operation and are normalized by the canopy height ( $h$ ). The symbols represent the data, and the lines are parabolic spline fits. No leaves: red line with square symbols; with leaves: green line with triangles.

**THE SITE.** With help and equipment largely from the NCAR’s In Situ Sensing Facility, CHATS took place in one of Cilker Orchards’s walnut (*Juglans regia*) blocks in Dixon, California (Fig. 1). We chose this location and orchard for many reasons, but the main factors were the size, age, and management practices of the orchard combined with consistent wind direction and speed. The CHATS instrumentation focused largely on the eastern section of this portion of Cilker Orchards. In this section, the trees were all walnuts of the Chandler variety. South of the main section of interest is a mix of slightly younger walnuts of mixed Chandler and Tulare variety, which is not owned by the Cilker family and is therefore managed independently. The western section of the Cilker’s block is also walnuts but consists mostly of the Howard variety and transitions to a small section of the Tulare variety in the very northwest corner. The section in the southwest quadrant contains almonds (*Amygdalus communis L. var. dulcis*) and is also independently managed.

mean wind direction to be fairly consistent: 50% from the north and 50% from the south with a small westerly component. We chose to focus on winds from the south because the CIMIS data also show that winds from the south tend to be weaker in magnitude with smaller direction variability, providing the potential for sampling a greater range of stability. For maximum fetch (~150 times the canopy height), the main towers were located near the northernmost border of the section (Fig. 1). This fetch should be ample for most of the sensors, except perhaps for the uppermost sensors during the most stably stratified periods (e.g., Baldocchi 1997; Rannik et al. 2000).

The campaign took place over 12 weeks in the spring of 2007 and was broken into three 4-week phases. Intensive measurements occurred during phase 1 (15 March–13 April), focusing on the walnut trees before leafout. Measurements continued but were unattended during the 4-week transition period of 14 April–13 May. After leafout, intensive measurements then resumed during phase 2 (13 May–12 June), focusing on the impact of the leaves on the flow dynamics, stability, and source/sink distribution of the scalars.

The trees in our section were planted in a nearly square pattern, such that they were about 6.9 m apart in the north–south direction and 7.3 m in the west–east direction (Fig. 2). The trees were all about 25 years old with an average height ( $h$ ) of about 10 m. The horizontal distribution of the vegetation was nearly homogeneous with the exception of an occasional tree that had been lost and replanted. The vertical plant area index (PAI) profile (square meter of plant area per square meter of ground area) was measured regularly through the campaign using a Li-Cor LAI-2000. Before leafout, the cumulative PAI was about 0.7, while following leafout the PAI increased to about 2.5. Figure 3 shows the average vertical profile of normalized plant area density (PAD; square meter of frontal plant area per cubic meter of air) both before and after leafout.

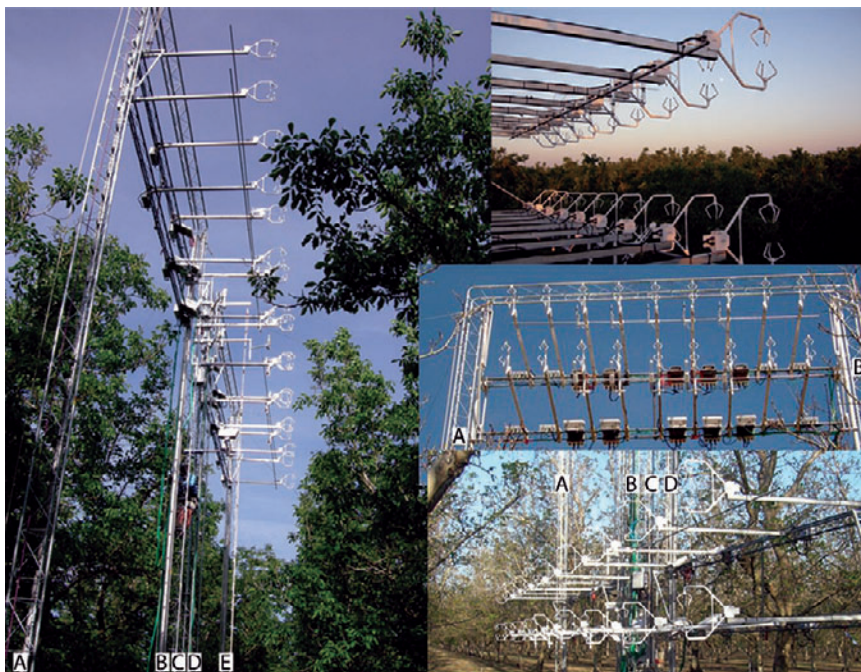


**FIG. 4.** Pictures of the CHATS array: (left) wide/high arrangement with leaves; (upper right) narrow/high arrangement with leaves; (middle right) wide/high arrangement with no leaves; (bottom right) wide/low arrangement with no leaves. The towers are marked A–E from west to east.

#### **OBSERVING THE CANOPY SCALES AND SMALLER.**

Within the orchard, the instrumentation was located in two main arrangements: a 30-m vertical tower and a horizontal array. Both were centered (in the west–east direction) within the Cilker’s walnut block, with the 30-m tower located about 100 m south from the northernmost edge of the section and the horizontal array another 100 m south from the tower (Fig. 1).

*The horizontal array.* The horizontal array consisted of five 12-m-tall towers oriented across the mean wind. The towers were situated such that three middle towers (labeled B, C, and D in Fig. 4) were 1.72 m apart, spanning a row with the middle of these three towers (C) centered within the row. Two additional towers were placed in adjacent tree rows [one in the row to the west (A), and the other to the east (E)]. Therefore, the entire array spanned three tree rows (two row middles).

On each of the four outermost towers, rails were attached to allow carriages to move vertically on the towers. The carriages were designed and manufactured by the NCAR Earth Observing Facility’s Design and Fabrication Services, which consisted of vertical members at each end connecting two horizontal tower members that were separated vertically by 1 m, where

this separation remained fixed during the experiment and was chosen with the intention to mimic typical canopy LES resolutions and to resolve the sharp vertical gradient in streamwise velocity at canopy top. The carriages were attached to ropes and pulleys so they could be easily raised or lowered to any location from the ground up to slightly above the canopy top. This flexibility facilitated rapid modification of the instrument arrangement with minimal impact on normal orchard operations.

The two horizontal sensor distributions were chosen, with separations of 0.5 and 1.72 m, such that when using a five-point filter (e.g., Sullivan et al. 2003; Horst et al. 2004), the filter scale determining the separation between resolved- and subfilter-scale motions would fall at 2 and 6.9 m, respectively. The 2-m filter width was chosen because it is typical of that used in canopy-resolving LES. The 6.9-m spacing was chosen for a number of reasons, including that this was the largest separation possible given the constraints imposed by the orchard operations and the length of the horizontal tower sections, and also to ensure that one filter width fell well within the energy-containing range of the turbulence and therefore averaged much of the canopy-induced scales of motion. In the “narrow” arrangement (0.5-m separation), all the sensors were located on a single carriage and therefore the sensors spanned between two tree rows or across a single row middle. With the “wide” arrangement (1.72-m separation), four sensors from each level moved to the adjacent carriage (to the east, spanning towers D and E) and the middle sensors shifted to the central tower (C). Figure 4 depicts the array setup in a variety of configurations.

The bottom row of the horizontal array included nine Campbell Scientific CSAT3 sonic anemometers measuring the three wind components plus sonic temperature at  $20 \text{ s}^{-1}$ . Collocated within the bottom row's central five CSAT3s, five Li-Cor 7500 sensors measured  $\text{CO}_2$  and  $\text{H}_2\text{O}$  fluctuations at  $20 \text{ s}^{-1}$ . The top row also included nine CSAT3 sonic anemometers, which were complemented by five Campbell Scientific KH20 Krypton hygrometers collocated within the central five sonic anemometers sampling water vapor density fluctuations at  $20 \text{ s}^{-1}$ . Also mounted within the upper five central CSAT3s were five Dantec Dynamics constant temperature single-wire hot-film anemometers (Model 55R01) oriented vertically and sampling wind velocity at  $2000 \text{ s}^{-1}$ . Two NCAR–Vaisala hygrometers [temperature/relative humidity (TRH)], one at each height of the array, measured mean aspirated

temperature and relative humidity at  $2 \text{ s}^{-1}$ . These instruments were all oriented toward the south on 1.5-m-long booms. All instruments were calibrated at NCAR's Calibration Laboratory before and after the experiment.

During the experiment, the horizontal array configuration was modified every five to seven days. These transitions included carriage heights and horizontal sensor separations. To properly characterize the impact of leaves on the turbulent momentum and scalar fluxes, we repeated each arrangement during both phases of the experiment (i.e., no leaves and with leaves).

During each phase, measurements were taken with the instrumentation in six different configurations (the narrow and wide horizontal separations at each of three heights: low, 2.5 m; middle, 6 m; and high, 10.1 m). The high location was chosen because it is the region of highest vertical shear of the streamwise velocity and hence where the majority of the momentum is extracted by the canopy. The middle height was located as close as possible to the within-canopy streamwise velocity minimum where wake-scale motions are expected to be particularly important in momentum transport and where the canopy-imposed scalar source/sink maximum occurs. The low height was chosen deep within the canopy at a height where the momentum transfer was expected to be largely a result of canopy-scale coherent structures and to be countergradient (i.e., centered at about 2.5 m where the mean velocity gradient is positive upward but turbulent momentum transfer is downward).

More than 1100 half-hour periods with good wind directions ( $\pm 30^\circ$  of directly into the array) with mean wind speeds above  $0.01 \text{ m s}^{-1}$  were collected during the campaign. Table 1 breaks these periods down into their various deployment heights, filter widths, leaf states, and atmospheric stability. At least 13 half-hour periods were obtained for any arrangement, while a single arrangement sampled up to 316 acceptable periods. Each deployment also sampled a wide range of atmospheric stability.

One key aspect of the CHATS campaign is the ability to investigate relationships between SFS fluxes of passive and active scalars that are largely absorbed/emitted by either the ground or by the canopy. Sample time–space plots of SFS scalar fluxes [one from a period when the canopy is leafless and largely dormant (Fig. 5) and the other from a period when the canopy is in full leaf and is actively transpiring (Fig. 6)] reveal that in this spectral range (scales smaller than the  $\sim 6.5$ -m filter),  $\text{CO}_2$  and  $\text{H}_2\text{O}$  fluxes

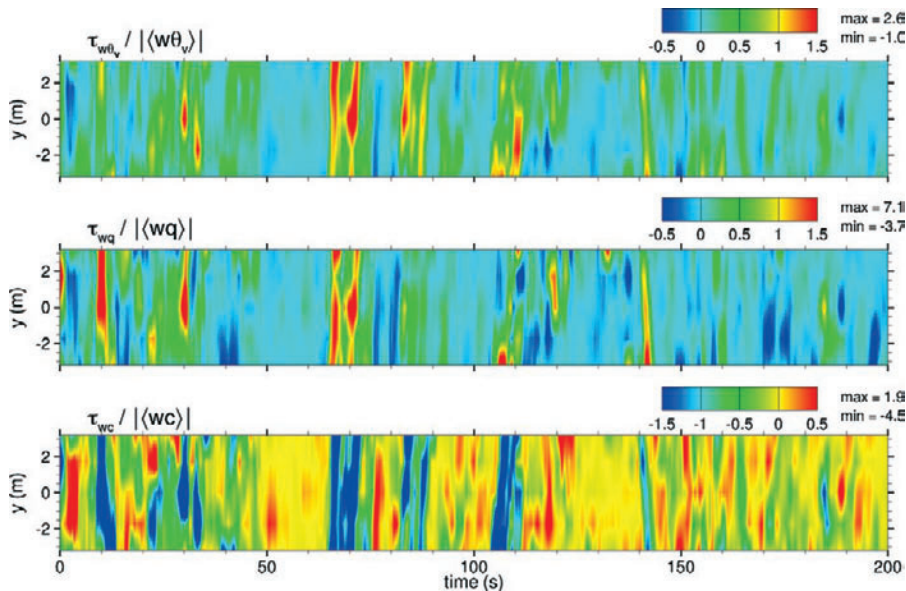
**TABLE 1.** The number of 0.5-h periods obtained during the CHATS campaign with mean wind directions from  $\pm 30^\circ$  directly into the array and above a minimum mean wind speed threshold of  $0.01 \text{ m s}^{-1}$ . The periods are broken down into the leaf state, array width, and array height characteristic of the canopy and array state during which the data were taken. This information is presented in the first three columns. The total number of “good” periods for each of these characteristics is presented in the rightmost column. The total number of periods for each of these characteristic states is further broken down into stability-class regimes defined by the height of the measurement ( $z$ ) and the locally evaluated Monin–Obukhov length

$$L = -\frac{g}{T} \frac{u_*^3}{kQ},$$

where  $g$  is the gravitational acceleration,  $T$  is a reference temperature,  $u_*$  is the friction velocity,  $k$  is the von Kármán constant, and  $Q_*$  is the buoyancy flux). Each stability-class regime presents two columns. The first column is the number of periods where  $z/L$  measured at the canopy top ( $z = h$ ) falls into this regime (left side of each bin class), and the second column is the number of periods where  $z/L$  measured at the height of the array ( $z = z_0$ ) falls into this regime (right side of each bin class, and in parentheses). Note that for each stability class, the left and right columns are the same when the array is in the uppermost position.

Leaf state	Width (m)	Height (m)	Number of 0.5-h periods with $z/L$ of													Total No. of periods
			-10	-10 to -5	-5 to -1	-1 to 0	0 to 1	1 to 5	5 to 10	10+						
No leaves	0.5	2.5	0 (0)	0 (1)	1 (0)	1 (2)	1 (0)	4 (1)	4 (0)	2 (9)	13					
No leaves	0.5	6.4	0 (0)	0 (1)	5 (5)	21 (21)	18 (14)	15 (15)	5 (7)	2 (3)	66					
No leaves	0.5	10.1	0 (0)	0 (0)	8 (8)	8 (8)	21 (21)	15 (15)	3 (3)	4 (4)	59					
No leaves	1.72	2.5	0 (9)	0 (7)	1 (6)	7 (6)	21 (2)	9 (4)	0 (1)	0 (3)	38					
No leaves	1.72	6.4	0 (0)	1 (1)	7 (12)	14 (9)	29 (25)	9 (11)	0 (2)	0 (0)	60					
No leaves	1.72	10.1	3 (3)	2 (2)	1 (1)	3 (3)	15 (15)	17 (17)	6 (6)	4 (4)	51					
Leafout	1.72	10.1	1 (1)	8 (8)	24 (24)	57 (57)	67 (67)	106 (106)	26 (26)	27 (27)	316					
Leaves	0.5	2.5	0 (7)	0 (10)	0 (10)	5 (3)	19 (5)	16 (5)	5 (3)	0 (2)	45					
Leaves	0.5	6.4	0 (0)	0 (1)	4 (8)	8 (19)	38 (20)	12 (14)	0 (0)	0 (0)	62					
Leaves	0.5	10.1	0 (0)	0 (0)	13 (13)	30 (30)	50 (50)	12 (12)	3 (3)	0 (0)	108					
Leaves	1.72	2.5	0 (3)	0 (22)	2 (25)	13 (5)	43 (7)	13 (8)	0 (0)	0 (1)	71					
Leaves	1.72	6.4	0 (0)	0 (0)	1 (5)	12 (9)	14 (12)	36 (32)	3 (3)	3 (8)	69					
Leaves	1.72	10.1	1 (1)	0 (0)	16 (16)	26 (26)	36 (36)	53 (53)	11 (11)	4 (4)	147					
Total No. of periods			5 (24)	11 (53)	83 (133)	205 (198)	372 (274)	317 (293)	66 (65)	46 (65)	1105					





atmospheric stability ( $h/L$ ) was  $\sim -0.04$ . The SFS fluxes are calculated using ID top-hat filtering in the  $x$  direction, where the filter width matches the sonic spacing in the  $y$  direction after the data are rotated into the mean wind direction (in this case, 6.8 m).

are shown to be negatively correlated independent of the leaf state, and after leafout the relative magnitude of the fluxes increases. Future analysis will involve dissecting the impact of stratification and scalar source/sink distributions on scale interactions within canopy flows and development and testing of parameterizations representing this complex regime.

*The 30-m tower. VELOCITY, TEMPERATURE, AND MOISTURE.* Thirteen main measurement levels tightly focused at the canopy top and growing in vertical separation with distance away from this focal point permitted the 30-m tower to sample the canopy-induced mechanical and thermodynamical vertical variation of turbulence transport characteristics and the linkages

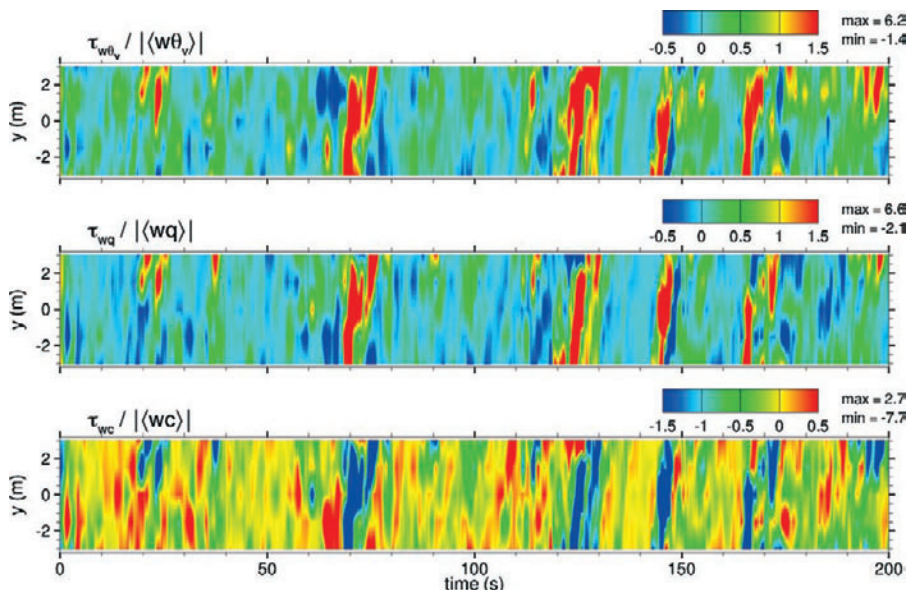


FIG. 6. As in Fig. 5, but at 0041 UTC 13 May 2007. This image comes from a period when leaves were on the trees (in full leaf) and actively transpiring. At the canopy top,  $u_*$  was  $0.78 \text{ m s}^{-1}$  and  $h/L$  was  $\sim -0.01$ . Mean wind direction in this case is 6.3 m.

FIG. 5. Sample time and space evolution of SFS fluxes of (top) virtual temperature ( $\tau_{w\theta_v}$ ), (middle) water vapor mixing ratio ( $\tau_{wq}$ ), and (bottom)  $\text{CO}_2$  ( $\tau_{wc}$ ) from the lower level of the array (9.6 m) at 0007 UTC 4 Apr 2007, when the array was deployed in the wide arrangement at the canopy top. The SFS fluxes have been normalized by the absolute value of the total flux of each averaged across all the sensors and 15 min. These observations were taken during a period when no leaves were on the trees. At the canopy top,  $u_*$  was  $0.68 \text{ m s}^{-1}$  and the

between canopy-scale motions and the larger-scale PBL turbulence. Six of these 13 levels were placed below the canopy top to capture the within-canopy impacts and six were placed above the canopy with the uppermost height nearly reaching the roughness sublayer height (29 m or about  $2.9h$ , where canopy effects should be minimal; Fig. 7).

Each of the 13 primary measurement levels contained 1) a Campbell Scientific CSAT3 sonic anemometer measuring all three wind components and virtual temperature

at  $60 \text{ s}^{-1}$  and 2) an NCAR–Vaisala hygrothermometer (TRH) measuring mean aspirated temperature and relative humidity at  $2 \text{ s}^{-1}$ . At six levels (deployed at every other level), Campbell Scientific KH2O Krypton hygrometers sampled water vapor density fluctuations at  $20 \text{ s}^{-1}$ . To maximize the acceptable wind directions and to minimize tower effects, the CSAT3s and Krypton hygrometers were deployed on 1.5-m booms directed to the west. The TRHs were deployed on similar booms pointing to the east to minimize their influence on the turbulence measurements. Example profiles (Fig. 8) illustrate the ability of the sensor deployment strategy on the 30-m tower to capture the aforementioned vertical stratification induced by interactions between the atmosphere, the land surface, and the vegetation canopy. As with the instruments in the array, all instruments on the tower were intercalibrated at the NCAR calibration facility prior to and again following the experiment.

Mounted on the sonic anemometers and pointed southward (Fig. 9), Dantec Dynamics constant temperature triple-wire hot-film anemometers (model 55R91) at three levels (midcanopy, 6 m; canopy top, 10 m; and above canopy, 14 m) sampled high-frequency finescale velocity fluctuations at  $2000 \text{ s}^{-1}$ .

**PRESSURE FLUCTUATIONS.** Measurements of turbulent pressure fluctuations ( $p'$ ) were made during CHATS. Quad-disk ports (Nishiyama and Bedard 1991)

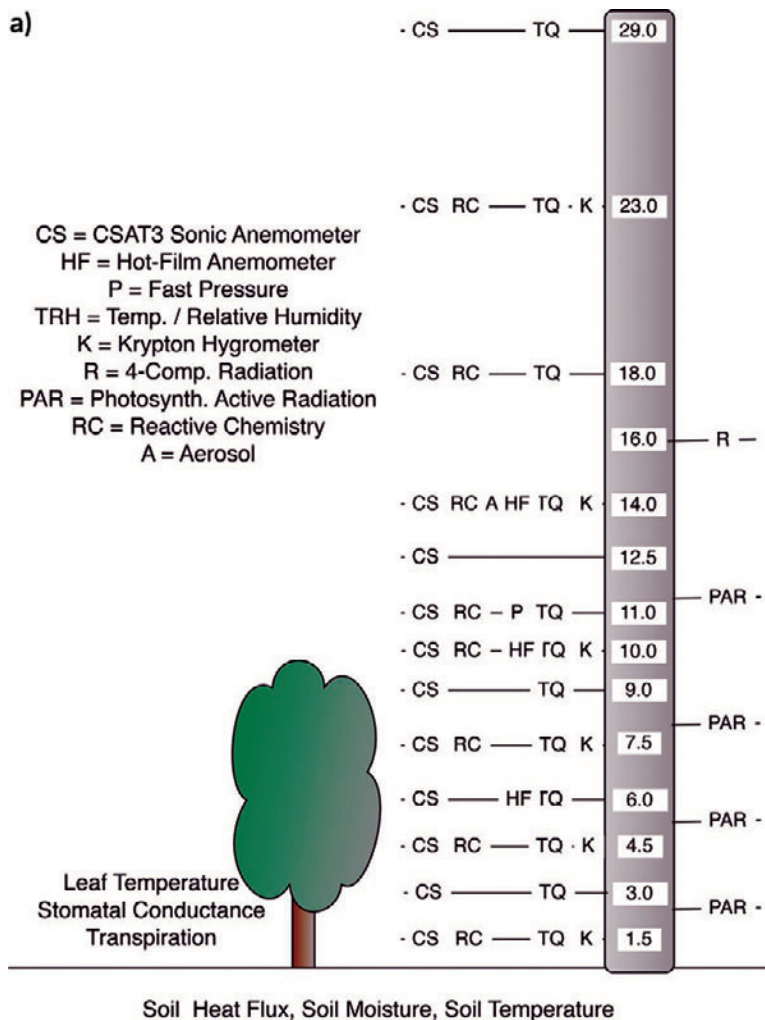


**FIG. 7. (a) Thirty-meter tower sensor configuration. Numbers on gray tower are in meters. Pictures of the 30-m tower from below: (b) no leaves and (c) with leaves.**

were used to minimize dynamic pressure errors (Fig. 9), where ports made by the National Oceanic and Atmospheric Administration's (NOAA) Environmental Technology Laboratory were chosen based on wind tunnel testing of three versions of this design.

Two types of pressure sensors were used: one similar to NOAA's sensor described by Wilczak and Bedard (2004) that uses an analog transducer (Furness Controls FCO44) and a reference volume with a calibrated leak, and a second newly designed NCAR sensor that uses a digital transducer (Paroscientific 202BG) and a fixed reference volume with a large thermal time constant to minimize the time rate of change of the reference pressure. A third, slower response sensor (Vaisala PTB220B) was also deployed to verify the  $p'$  sensor operation at low frequencies.

Before being placed in their final locations, the systems were connected to a single inlet probe installed at 11 m on the 30-m tower (where the turbulence intensities diminished substantially from that found within the canopy) and were determined to

be operating properly by investigating the horizontal heat flux budget, as suggested by Wilczak and Bedard (2004). During phase 2, the NCAR pressure sensor and an additional quad-disk probe were shifted into the horizontal array. Future analysis includes 1) comparing these measurements to canopy flow models describing the variation of pressure transport of turbulent kinetic energy (TKE) at the different heights within and near the canopy and 2) investigating the pressure destruction term in the filtered scalar flux equation that is modeled in LES.

RADIATION, SOILS, PRECIPITATION, AND IRRIGATION. For the entire campaign, two Kipp and Zonen CM21 pyranometers and two Kipp and Zonen CG4 pyrgeometers were deployed at 16 m to measure the broad spectrum downwelling and upwelling above-canopy radiation. A similar Eppley four-component system [with Precision Spectral Pyranometer (PSP) and Precision Infrared Radiometer (PIR) sensors] deployed two tree rows to the west at a height of 2 m captured the subcanopy radiational forcing. A

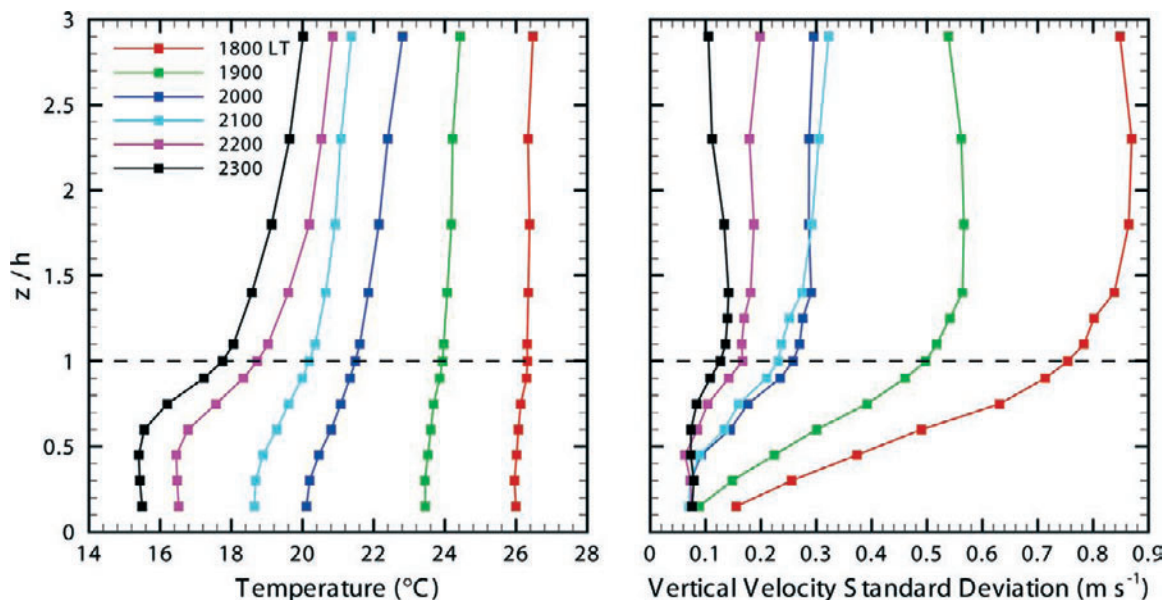


**FIG. 8.** The time evolution of hourly-averaged (left) temperature and (right) vertical velocity standard deviation profiles during the evening transition of 21 May while the canopy is in full leaf. The 30-m tower deployment strategy captures the time evolution of vertical stratification variations induced by interactions among the atmosphere, land surface, and the vegetative canopy. Between 1900 and 2000 LT, the solar forcing diminishes and the air near the surface begins to cool first. By 2300 LT, the upper canopy absorbs and reemits the outgoing radiation back to the ground surface, keeping the lower canopy air warm while the leaves cool due to their exposure to the overlying atmosphere and the loss of their emitted thermal radiation. At 2300 LT, the lower canopy ( $z/h < 0.5$ ) is therefore unstably stratified, which vertically mixes surface-emitted quantities through this depth (note the coincident relative increase in vertical velocity fluctuations at this time). Conversely, the upper canopy layers ( $0.5 < z/h < 1.0$ ) are dramatically more stable than the overlying atmospheric layers, which limits turbulent exchange between the within-canopy and above-canopy regions, and sets up ideal conditions for gravity wave formation (e.g., Fig. 13).

Micromet Systems Q7 net radiometer also installed at this location complemented the Eppley subcanopy four-component radiation measurements. During phase 2 of the experiment, a single Li-Cor LI-190 above the canopy and three Li-Cor LI-191 line sensors measured photosynthetically active radiation (PAR) at four heights (2, 5, 8, and 12 m). All radiation measurements were sampled at  $1 \text{ s}^{-1}$ .

Located 2 m from the subcanopy radiation measurements, observations of soil moisture, soil temperature, soil heat flux, and soil thermal conductivity, diffusivity, and heat capacity were made at 0.05-m depth and at 1 Hz using a Decagon ECH<sub>2</sub>O soil moisture sensor, a Radiation and Energy Balance Systems (REBS) soil temperature sensor, a REBS HFT-3 soil heat flux sensor, and a Hukseflux TP01 thermal properties sensor, respectively. A collocated tipping-bucket rain gauge deployed at 1-m height (above the orchard sprinklers) captured precipitation. During phase 2, three complete irrigation cycles occurred in a rotating fashion through the orchard block. The sprinkler system irrigated for 24 consecutive hours per circuit, completing a complete irrigation cycle in six days.

**REACTIVE CHEMISTRY.** Most previous studies assume negligible chemical effects (either losses or production) on the measured eddy fluxes of ozone above canopies (e.g., Mikkelsen et al. 2000). However, recent studies imply that up to 50% of the ozone deposition observed may be explained by fast chemistry between ozone and reactive odd nitrogen and volatile organic species occurring near or within the canopy (e.g., Kurpius and Goldstein 2003).

During phase 2, mean vertical profiles of O<sub>3</sub> (2B Technologies 205), NO, and NO<sub>x</sub> (Eco Physics CLD88 Y) measured at 1.5, 4.5, 9, 11, 14, and 23 m (e.g., Fig. 10) along with two levels of disjunct eddy covariance<sup>2</sup> ozone flux measurements above the canopy (14 and 23 m) can be used to determine the impact of fast chemistry on ozone flux. Since no chemical effects upon H<sub>2</sub>O are expected, observed H<sub>2</sub>O fluxes serve as a control measurement for deducing vertical divergences in the flux due to factors other than chemistry (assuming each has similar source distributions).

Gradient measurements of volatile organic compounds were performed using an Ionicon proton-



**FIG. 9. Photograph of the quad-disk pressure port when the second pressure port was vertically centered within the array. Note the single-wire hot-film anemometer mounted within the upper CSAT3 sonic anemometer and the krypton hygrometer located behind.**

transfer-reaction mass spectrometer (PTR-MS).<sup>3</sup> On three days, selected VOCs were measured with fast response at three levels (4.5, 9, and 11 m). The PTR-MS has a time response suitable for eddy covariance measurements (e.g., 10 Hz; Karl et al. 2000) and is used extensively for eddy covariance measurements (Rinne et al. 2001; Karl et al. 2002; Ammann et al. 2004; Spirig et al. 2005; Lee et al. 2005). The impact of within-canopy chemical processing on canopy VOC emission strength estimates will be assessed for a variety of VOCs and compared with future LES calculations.

Surprisingly, and for the first time, high levels (up to 120 pptv) of methyl salicylate [MeSA; C<sub>6</sub>H<sub>4</sub>(HO)

<sup>2</sup> Disjunct eddy covariance is a method for estimating scalar fluxes using sensors that are not of adequate frequency response for straightforward flux measurement (Lenschow et al. 1994).

<sup>3</sup> PTR-MS employs a soft ionization technique that preserves important information of the measured compound reflected in the corresponding molecular ion. PTR-MS allows for the quantitative online detection of VOCs down to pptv-level concentrations (Lindinger et al. 1998; Hansel et al. 1995; de Gouw et al. 2003) without any preceding sample treatment.

COOCH<sub>3</sub>] were detected in ambient air. PTR-MS mass scans were confirmed by gas chromatograph mass spectrometer (GC-MS) analysis. Profile measurements show a distinct source of methyl salicylate from the canopy. Methyl salicylate activates specific defense genes through the salicylic acid pathway and is thought to act as a volatile signaling molecule when plants are under stress or herbivorous attack. Methyl salicylate emission by the Chandler walnuts during CHATS was found to correlate with water and temperature stress (Karl et al. 2008).

**AEROSOLS: TURBULENT FLUXES AND PARTICLE SIZE DISTRIBUTION.** Particle number concentrations were measured with a condensation particle counter (CPC 3772, TSI Inc.) installed on the 30-m tower with the inlet mounted adjacent to the 14-m sonic anemometer. Aerosol data were sampled at 10 Hz with an instrument time constant of 0.42 s. Turbulent aerosol number fluxes can be calculated by direct eddy covariance and also by simulated relaxed eddy accumulation (REA; Businger and Oncley 1990). Recent analysis of these aerosol data suggests that the use of

temperature or water vapor concentration as a proxy scalar to derive the *b* factor<sup>4</sup> for REA is no better than assuming a constant value for *b* (Held et al. 2008).

For additional physical characterization (e.g. identification of particle formation events, general aerosol burden), particle size distributions were measured for diameters ranging from 10 nm to 2 μm using a scanning mobility particle sizer (SMPS; TSI Inc.), a condensation particle counter (CPC 3760, TSI Inc.), and an optical particle counter (LASAIR, Particle Measuring Systems), sampling below the canopy at 2 m. During the day, aerosol concentrations reached 12,000 particles cm<sup>-3</sup>, decreasing to 3,000 particles cm<sup>-3</sup> at nighttime.

**Leaf-level characterization.** Enclosure systems are used to identify the ecosystem components controlling gas and aerosol exchange and to develop quantitative parameterizations that can be used in bulk canopy-scale flux models. VOC, CO<sub>2</sub>, and H<sub>2</sub>O fluxes from various walnut tree tissues (walnuts, leaves, and stems were observed during CHATS using the enclosure technique). The system included

<sup>4</sup> Here *b* is a proportionality factor relating the turbulent flux of an atmospheric constituent to the product of the vertical velocity standard deviation and the concentration difference between two reservoirs when the flow rate into these reservoirs is kept proportional to the vertical wind speed (Businger and Oncley 1990).

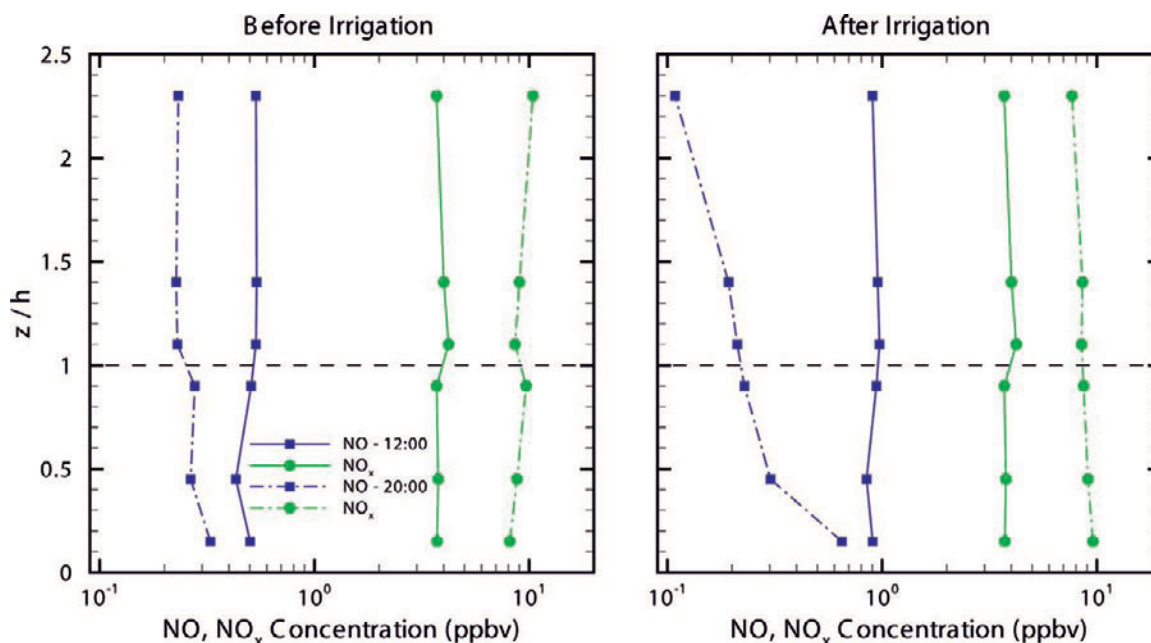


**FIG. 10.** Sample profiles of 1-h averaged NO and NO<sub>x</sub> concentrations (ppbv). (left) Profiles of 1-h averages centered on 1200 and 2000 LT and over the period from 13 to 21 May immediately preceding the first irrigation cycle. (right) As at (left), but from the period immediately following irrigation (26 May–5 Jun). Note the evening increase in near-surface NO<sub>x</sub> resulting from the postirrigation increase in available soil water, consistent with Williams et al. (1992).

a Li-Cor 6400 leaf cuvette, a 500-ml glass enclosure, and a 5-L Teflon bag enclosure. Fluxes of CO<sub>2</sub> and H<sub>2</sub>O were quantified using an infrared gas analyzer. VOCs were analyzed using three complementary approaches: 1) the PTR-MS quantified a large range of biogenic VOCs, 2) an in-situ GC-MS quantified and identified most of the important biogenic VOCs, and 3) samples were collected on solid adsorbent tubes and transported to a highly sensitive laboratory Gas Chromatograph with Massachusetts Spectrometer and Flame Ionization Detector (Agilent 5975C) system to quantify trace constituents.

A Li-Cor 6400 system investigated the response of VOC, CO<sub>2</sub>, and H<sub>2</sub>O fluxes to variations in leaf temperature and incident radiation. Individual leaves tested using this system included shaded and sunlit leaves as well as young and mature leaves. Using the glass enclosure, emissions from undisturbed and wounded walnuts were examined.

The Teflon bag enclosure investigated emissions from stems and leaves, including both undisturbed and wounded tissues. Relatively low terpenoid and green leaf volatiles (GLV) (e.g., hexenol, hexenal) emissions were observed from undisturbed leaves, stems, and walnuts (Fig. 11). Substantial emissions of green leaf volatiles and dimethyl-nonatriene (DMNT) were observed from wounded leaves. A large number of monoterpenes (MT) and sesquiterpenes were emitted from both leaves and walnuts when they were wounded. These leaf-level observations will be used to test canopy-resolving land surface models (e.g., Patton et al. 2008) and to assess impact of within-canopy chemistry on source/sink estimates based upon ecosystem-level observations and inverse Lagrangian models (e.g., Karl et al. 2008).

**Thermal imagery.** To measure heat storage in the biomass and to determine the boundary conditions for heat exchange between vegetation and soil surfaces and atmosphere, a FLIR ThermaCAM SC3000 IR camera was deployed at the CHATS field site. The camera was mounted atop the horizontal array structure at a height of 12 m, looking

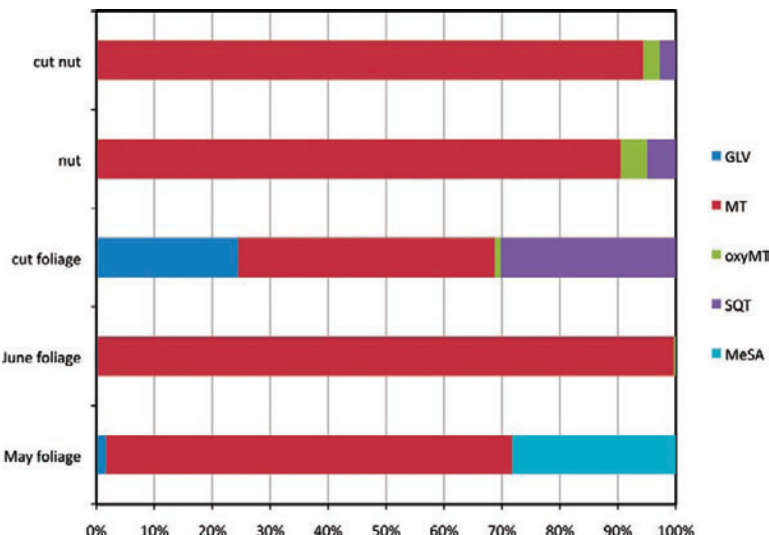


**FIG. 11. A comparison of emissions from undisturbed and wounded walnuts and leaves. The different colors depict (i) GLV consisting primarily of Z-3-hexenal, Z-3-hexenol with some contribution from E-2-hexenal, and 3-1-hexenol acetate; (ii) MT, consisting primarily of beta-pinene, alpha-pinene, d-limonene, cis-beta-ocimene with some contribution from tricyclene, camphene, sabinene, a-terpinene, and a-phellandrene; (iii) oxygenated MT (oxyMT), consisting primarily of 1,8 cineole with some contribution from linalool, pinocarveol, and bornyl acetate; (iv) sesquiterpenes, consisting primarily of beta-caryophyllene and cedrene; and (v) MeSA. Of importance is that the May foliage samples are preirrigation, while the June foliage samples are postirrigation.**

south-southeast from 12 May to 7 June. The camera was mounted on a tripod located 5 m south of the center of the horizontal array at a height of 1.67 m from 8 to 10 June. A second thermal camera (FLIR ThermaCAM PM380) was deployed throughout the orchard in a semirandom fashion and hand-held images were collected.

The SC3000 IR camera measures radiance at 8- $\mu$ m wavelength and was equipped with a wide-angle lens with a field of view of 45° × 60° and 240 × 320 pixels. The radiational accuracy of the camera is 1%. Images were acquired every 2 min. Figure 12 shows a typical IR image. After applying an image processing algorithm to determine the pixels associated with trunk and leaves, the diurnal cycle of trunk and leaf surface temperatures can be obtained (see Fig. 12 for an example time series). Improper accounting for biomass heat storage can produce significant error in short time-scale energy budget closure since trunk temperature can lag air temperature by several hours (e.g., Haverd et al. 2007); this dataset should permit development and evaluation of these models and improve their ability to predict energy partitioning (e.g., Garai et al. 2010).

*Turbulent diffusion measurements; Trace Gas Automated Profiling System (T-GAPS).* To improve our understanding and predictive capability of diffusion in canopy turbulence, a dispersion experiment took place during CHATS. The experiment consisted of an SF<sub>6</sub> line source located 40 m south of the 30-m tower and a meter above the ground, oriented in the east–west direction. Nine strategically placed syringe samplers mapped out the along-wind surface concentrations. To capture the vertical dispersion, the Washington State University Trace Gas Automated Profiling System [T-GAPS, which was previously called the Tracer Vertical (TRAVERT) system; see Flaherty et al. 2007] continuously sampled from lines on the 30-m tower. The T-GAPS system automatically collects and analyzes 5-min averaged whole air samples obtained simultaneously through seven long sample lines.

One of the key aims of the dispersion experiments and analysis is to determine the canopy-induced stability effects on turbulent dispersion, especially at night, when the lower canopy layers are unstable but the upper and above-canopy layers are stable (Fig. 8; 2300 LT). Much of the analysis will be done in conjunction with a Lagrangian particle dispersion model (Weil et al. 2004). This turbulent dispersion analysis will also help determine the biological significance of plant-to-plant communication in the atmosphere (see, e.g., the “Reactive chemistry” section; Shulaev et al. 1997).

**OBSERVING THE CANOPY SCALE, ORCHARD SCALE, AND LARGER.** *High-resolution aerosol backscatter lidar.* The NCAR Raman-

shifted Eye-Safe Aerosol Lidar (REAL) collected data from 15 March to 11 June from a site 1.6 km directly north of the 30-m tower. The instrument is described in detail in a series of papers (Mayor and Spuler 2004; Spuler and Mayor 2005; Mayor et al. 2007). REAL is an elastic backscatter lidar that operates at a wavelength of 1.5 μm in order to safely transmit high-energy laser pulses. For the CHATS deployment, REAL was upgraded for enhanced sensitivity to smaller-scale atmospheric features. The instrument’s receiver—specifically the transimpedance amplifier module—was redesigned to have a higher-frequency bandwidth. Laboratory measurements showed the upgraded detector/amplifier module had significantly better performance at higher frequencies (e.g., >3 dB improvement at 30 MHz.) This modification increased the spatial resolution so that during CHATS, REAL could sample and observe canopy-scale motions.

During CHATS, REAL operated at a pulse rate of 10 Hz and recorded backscatter data in 1.5-m range intervals. From its location, REAL was able to scan just meters above the canopy. More than 2,800 hours of data were collected during its deployment in CHATS. Both vertical and horizontal scans were collected. During periods of southerly winds, the scan strategy collected higher-angular-resolution data surrounding the towers (175°–185°); at other times, wider-angle scans were collected (151°–211°). REAL routinely observed good signal-to-noise aerosol backscatter data to ranges beyond 5 km.

The deployment of REAL at CHATS aimed to achieve multiple goals: 1) advancement of the instrument’s ability to create time-lapse visualizations

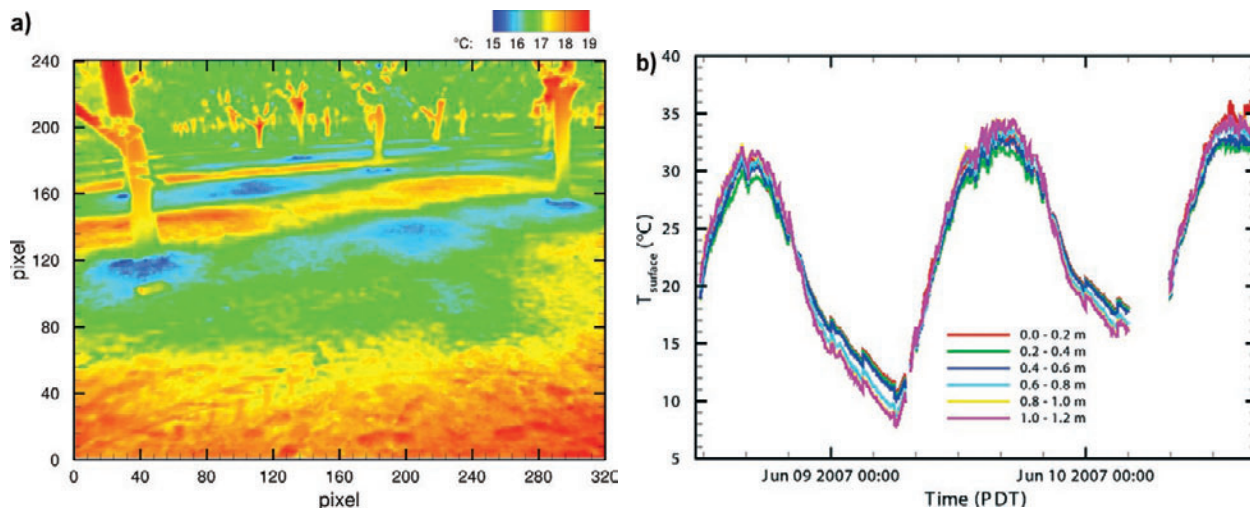


**FIG. 12.** (a) A nighttime IR image on 8 Jun. (b) Time series of average trunk temperature averaged over six heights for 8–10 Jun 2007. Note that during the daytime, the upper and lower tree trunk is warmer than the middle trunk levels; during nocturnal (predawn) conditions, the lower trunk cools the slowest.

of turbulent coherent structures, 2) collection of a dataset allowing one to relate changes in the lidar aerosol backscatter to several in situ measurements and to explore the use of the backscatter data for the remote measurement of scalar two-point turbulence statistics, 3) exploration of linkages between PBL-scale and canopy-scale turbulence, and 4) characterization of the local meso-gamma-scale structure of the atmosphere in which the CHATS in situ measurements were made. This includes monitoring boundary layer depth ( $z_b$ ) and deriving the vector flow field

via the correlation technique as done previously by Mayor and Eloranta (2001).

The REAL dataset from CHATS contains a number of interesting phenomena. Figure 13 presents examples of some of the key features observed, including (top left) a sea-breeze frontal passage, (top right) canopy-top gravity waves, and (bottom) horizontal and vertical high-resolution sampling of turbulent scales of motion above and within the orchard canopy. Initial analysis of the REAL datasets from CHATS is aimed at 1) characterizing entrainment

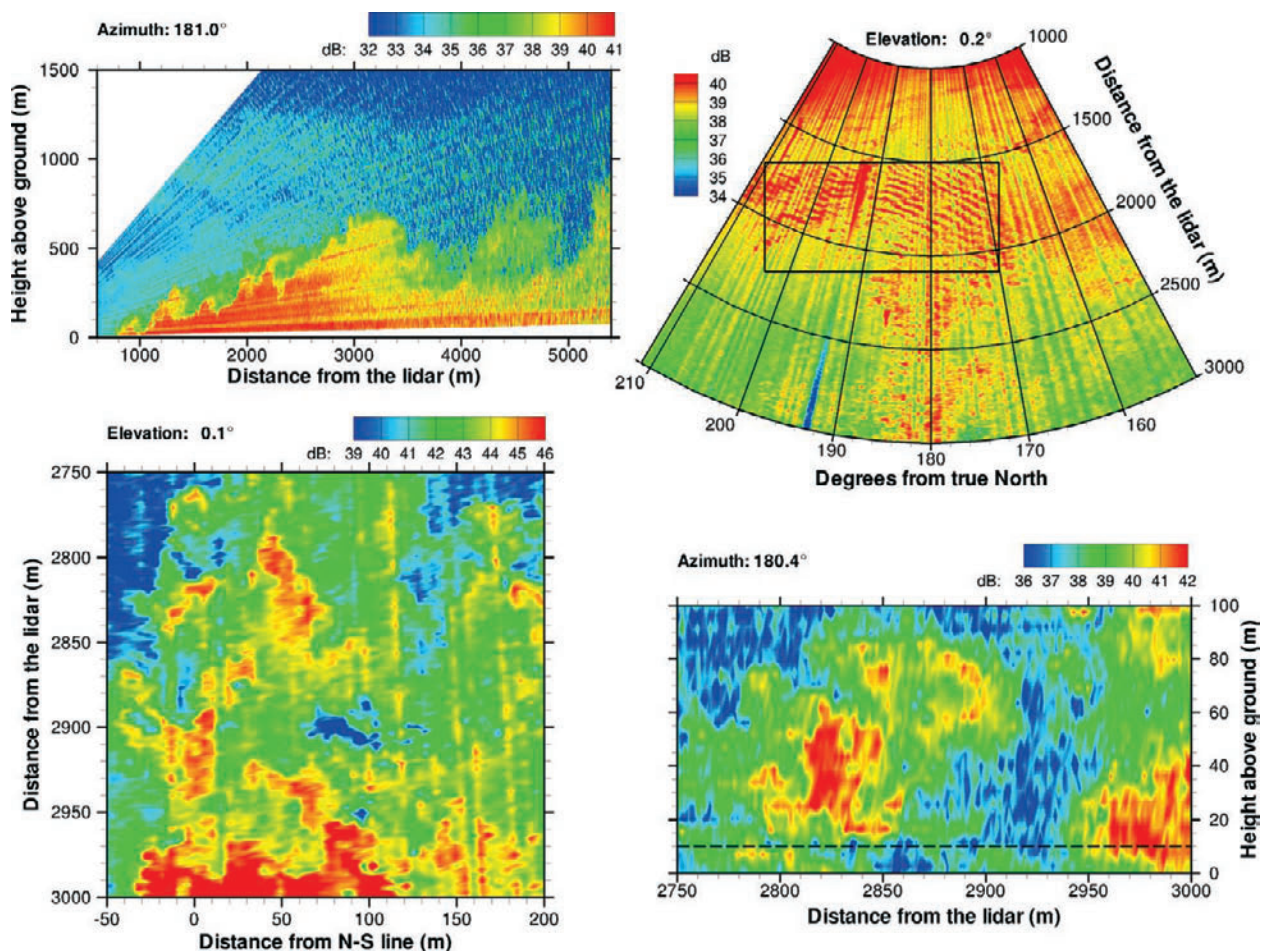


FIG. 13. Four images of aerosol backscatter intensity (dB) from REAL during CHATS. (top left) An RHI scan at 0111 UTC 1 May (1811 LT Apr 30) at azimuth  $181^\circ$  (or nearly due south) depicting the passage of a sea-breeze front traveling from right to left; note the evolving length scales (from left to right) participating in the entrainment process between the two different density fluids. (top right) A PPI scan at an elevation  $0.2^\circ$  above the horizontal taken at 1349 UTC 25 Apr (0649 LT 25 Apr) showing canopy-scale gravity waves induced by velocity shear and thermal stratification at the canopy top; Cilker Orchards is roughly contained within the rectangle. (bottom left) A near-horizontal PPI scan (elevation  $0.1^\circ$  above the horizontal). (bottom right) An RHI scan (azimuth  $180.4^\circ$  or nearly due south). These lower two panels focus in on the near-canopy region and therefore only depict a fraction of the total region scanned by REAL. The horizontal slice (bottom left) is from 2353 UTC 24 May (1653 LT 24 May), and the vertical slice (bottom right) is from 2344 UTC 24 May (1644 LT 24 May). The dashed line (bottom right) depicts the top of the canopy. Note that REAL was able to sample RHI slices down into canopy because of orchard pruning and that its high resolution permits sampling of canopy-scale motions as well as the full PBL-scale flow.



processes and translation speeds of sea-breeze fronts (e.g., Mayor 2011), 2) investigating spatial correlation length scales associated with canopy flows, 3) establishing criteria for the onset/propagation/decay of canopy-induced gravity waves, and 4) testing of vortex identification methods previously limited to turbulence-resolving numerical models (e.g., Finnigan et al. 2009). The REAL data from CHATS are available at [www.phys.csuchico.edu/lidar](http://www.phys.csuchico.edu/lidar).

**Coherent Doppler lidar.** Arizona State University (ASU) deployed its Coherent Technologies WindTracer Doppler lidar during phase 2. The primary motivations of the ASU lidar deployment were to 1) illuminate the connection between the boundary layer scales of motion and canopy turbulence, 2) gather Doppler lidar data appropriate for analysis of data assimilation methods, 3) characterize small-scale winds and turbulence above the canopy, and 4) measure properties of boundary layer development, such as the evolution of the PBL height and aerosol levels.

The ASU lidar was located 2.05 km to the east with a clear line of sight of Cilker Orchards (Fig. 1). With an azimuthal angle of  $279^\circ$  and an elevation angle of  $0.75^\circ$ , the ASU lidar pointed at the top of the 30-m tower.

Generally, data quality was high and the planned scans for supporting the experiment were executed successfully. Acceptable quality was typically obtained for the lidar signal to a range of approximately 4 km, though this varied significantly depending on daily aerosol and humidity levels. Scanning strategies included mixed plan position indicators (PPIs)/range height indicators (RHIs), low-level PPIs for gust tracking, and fast volumetric scans in anticipation of data assimilation analysis using 4D variational methods. Some of the latter scans were timed to correspond with the helicopter deployment (see next subsection) that took place toward the beginning of phase 2.

**Helicopter observation platform.** The Duke University Helicopter Observation Platform (HOP; Avissar et al. 2009) also participated in CHATS. HOP consists of a Bell 206 Jet Ranger helicopter, equipped with a three-dimensional, high-frequency positioning and attitude recording system, a data acquisition and real-time visualization system, and fast response sensors to measure turbulent velocity and temperature (Kaijo USV, Aventech AIMMS-20), along with moisture and  $\text{CO}_2$  fluctuations (Li-Cor 7500). Thus, HOP can collect the variables needed to compute scalar fluxes (using the eddy-correlation technique) at low altitudes and low air speeds that are not feasible with airplanes,

yet are essential for studying the exchanges between the Earth's surface and the atmosphere (Avissar et al. 2009).

HOP flew during four different daytime periods. To characterize the large-scale PBL structure, the flight strategy for HOP involved profiling from just above the canopy to above the PBL depth in approximately 50-m increments. At each elevation, samples were taken for about a 3-km distance. Interspersed with these PBL profiles, HOP flew five west–east horizontal tracks sampling at five different north–south locations (one upwind, three over the orchard, and one downwind) across the orchard at an elevation of approximately 15 m (about 5 m above the tree tops). These five tracks provide a mapping of the spatial structure and the evolution across the orchard. Each complete set of samples (PBL profile plus canopy-top mapping) took a little more than an hour. Without refueling, HOP could complete three sets of horizontal passes over the orchard and two PBL profiles. In total, HOP sampled approximately 25 flight hours during CHATS. This data should provide unique insight into the PBL-canopy-scale coupling.

**Minisodar/RASS.** For the duration of the experiment, a minisodar was deployed 2 km east of the 30-m tower to monitor the lower boundary layer (Fig. 1). The sodar is a Metek DSDPA.90–24 phased array system with a radio acoustic sounding system (RASS) (Engelbart et al. 1999). Wind is measured using a Doppler scanning technique and virtual temperature using RASS with a collocated 915-MHz radar to trace the acoustic pulses (since the speed of sound is proportional to virtual temperature). The sodar produces reflectivity, wind, and virtual temperature profiles every 10 min from 40 m up to around 200 m in 20-m intervals. The system was able to trace the development of the nocturnal inversion and/or the early-morning convective boundary layer on most days.

**Scintillometers.** During phase 2, three Scintec BLS900 double-beam large-aperture scintillometer transects were deployed at several locations. The instruments were sampled at 5 Hz and 1-min averages of the refractive index structure parameter ( $\chi^2$ ) were recorded. One permanent transect of 647 m long was located 800 m north of the CHATS orchard over a sunflower field at an effective height  $z = 3.1$  m. Two additional transects were mobile and deployed at several locations, such as over the different fields nearby and across the walnut orchard below the leaves ( $z = 0.85$  m AGL). These observations are intended to permit investigating relationships such as between

time averages at single points and spatial averages across the transects.

**CONCLUDING REMARKS.** The CHATS program brought together an interdisciplinary group of scientists to investigate ecosystem–atmosphere exchange in an idealized setting: a horizontally homogeneous single-aged walnut orchard. The observations focused on measurements characterizing stratification influences on the spatial structure of canopy-induced turbulence, the trace gas source/sink distribution associated with vegetation, and the overall impact of canopy-induced processes on trace gas transport. The campaign design specifically aimed to connect observations directly with model development, testing, and understanding.

An important emphasis within the CHATS program includes the future community-wide availability of the data. The data will be made available via NCAR's Earth Observing Laboratory Web site (currently [www.eol.ucar.edu/chats](http://www.eol.ucar.edu/chats)). The CHATS dataset should provide community insight into canopy–atmosphere coupling for years to come. We hope that CHATS serves as a model for future instrument deployments, integrating fast eddy covariance measurements with canopy profiling in order to better understand within-canopy processes and their impact on measured fluxes.

**ACKNOWLEDGMENTS.** First, we would like to express our sincere gratitude to both the Cilker family and Antonio Paredes. All parties were extremely generous, tolerant, and accommodating during CHATS; we really appreciate that they took a sincere interest in the scientific outcome. Their friendly support and cooperation during the experiment was a critical component of the success of the experiment. We look forward to turning the science into practical information for them and the rest of the agricultural community.

Second, we would like to acknowledge the extremely skillful, timely, and understanding effort put forward by the NCAR Earth Observing Laboratory field and fabrication staff. The entire crew was a fantastic group to work with and was always willing to put the science first.

Joe Grant from the University of California, Cooperative Extension in Stockton, California, guided us during our search for an appropriate orchard and connected us with the Cilkers. Mario Moratorio and Paul Lum from the University of California, Cooperative Extension in Davis, California, provided advice on instrument location and helped establish contact with Bob Currey, Craig Gnos, and Roy Gill, who allowed us to place research equipment on their property.

Jan Hendrickx (New Mexico Tech) lent us the FLIR infrared camera and Mekonnen Gebremichael (University of Connecticut) lent one Scintec BLS900. Michael Sankur, Yoichi Shiga, Mandana Farhadieh, Anirban Garai, Dawit Zeweldi, and Erich Uher from UC San Diego assisted in the field.

We would also like to acknowledge our funding sources that came together to make this program happen. Most support came from two branches of the National Science Foundation Division of Atmospheric Sciences: 1) the Lower Atmosphere Observing Facilities program and 2) the National Center for Atmospheric Research's (NCAR's) Bio-Hydro-Atmosphere Interactions of Energy, Aerosols, Carbon, H<sub>2</sub>O, Organics and Nitrogen (BEACHON) program. EGP, PPS, JCW, RA, and RC gratefully acknowledge the support of the Army Research Office and the guidance of Program Manager Dr. Walter Bach (Contracts/Grants MIPR5HNS-FAR044, W911NF-04-1-0411, W911NF-09-1-0572, and W911NF-07-1-0137). EGP also acknowledges support from the Center for Multiscale Modeling of Atmospheric Processes (CMMAP) at Colorado State University, NSF Grant ATM-0425247, and Contract G-3045–9 to NCAR. AH was supported by a research fellowship of the German Research Foundation DFG (HE-5214/1-1). Other essential support came from Arizona State University, Duke University, and the University of California. S. D. Mayor acknowledges support from NSF AGS 0924407 to process and analyze the REAL data.

## REFERENCES

- Ammann, C., C. Spirig, A. Neftel, M. Steinbacher, M. Komenda, and A. Schaub, 2004: Application of PTR-MS for measurements of biogenic VOC in a deciduous forest. *Intl. J. Mass Spectrom.*, **239**, 87–101.
- Avisar, R., and Coauthors, 2009: The Duke University Helicopter Observation Platform. *Bull. Amer. Meteor. Soc.*, **90**, 939–954.
- Baldocchi, D. D., 1997: Flux footprints within and over forest canopies. *Bound.-Layer Meteor.*, **85**, 273–292.
- Belcher, S. E., J. J. Finnigan, and I. N. Harman, 2008: Flows through forest canopies in complex terrain. *Ecol. Appl.*, **18**, 1436–1453.
- Böhm, M., J. J. Finnigan, and M. R. Raupach, 2000: Dispersive fluxes and canopy flows: Just how important are they? *Extended Abstracts, 24th Conf. on Agricultural and Forest Meteorology*, Davis, CA, Amer. Meteor. Soc., 5.6. [Available online at [http://ams.confex.com/ams/AugDavis/techprogram/paper\\_15456.htm](http://ams.confex.com/ams/AugDavis/techprogram/paper_15456.htm).]
- Bonan, G. B., 2008: Forests and climate change: Forcings, feedbacks, and the climate benefits of forests. *Science*, **320**, 1444–1449, doi:10.1126/science.1155121.

- Businger, J. A., and S. P. Oncley, 1990: Flux measurement with conditional sampling. *J. Atmos. Oceanic Technol.*, **7**, 349–352.
- de Gouw, J. A., and Coauthors, 2003: Validation of proton transfer reaction-mass spectrometry (PTR-MS) measurements of gas-phase organic compounds in the atmosphere during the New England Air Quality Study (NEAQS) in 2002. *J. Geophys. Res.*, **108**, 4682, doi:10.1029/2003JD003863.
- Engelbart, D., H. Steinhagen, U. Gorsdorf, J. Neisser, H.-J. Kirtzel, and G. Peters, 1999: First results of measurements with a newly designed phased-array sodar with RASS. *Meteor. Atmos. Phys.*, **71**, 61–68.
- Feigenwinter, C., and Coauthors, 2008: Comparison of horizontal and vertical advective CO<sub>2</sub> fluxes at three forest sites. *Agric. For. Meteorol.*, **148**, 12–24, doi:10.1016/j.agrformet.2007.08.013.
- Finnigan, J. J., 2000: Turbulence in plant canopies. *Annu. Rev. Fluid Mech.*, **32**, 519–571.
- , R. H. Shaw, and E. G. Patton, 2009: Turbulence structure above a vegetation canopy. *J. Fluid Mech.*, **637**, 387–424.
- Flaherty, J. E., B. Lamb, K. J. Allwine, and E. Allwine, 2007: Vertical tracer concentration profiles measured during the Joint Urban 2003 dispersion study. *J. Appl. Meteor. Climatol.*, **46**, 2019–2037.
- Fuentes, J. D., and Coauthors, 2000: Biogenic hydrocarbons in the atmospheric boundary layer: A review. *Bull. Amer. Meteor. Soc.*, **81**, 1537–1575.
- Gao, W., R. H. Shaw, and K. T. Paw U, 1989: Observation of organized structure in turbulent flow within and above a forest canopy. *Bound.-Layer Meteorol.*, **47**, 349–377.
- Garai, A., J. Kleissl, and S. G. Llewellyn Smith, 2010: Estimation of biomass heat storage using thermal infrared imagery: Application to a walnut orchard. *Bound.-Layer Meteorol.*, **137**, 333–342, doi:10.1007/s10546-010-9524-x.
- Guenther, A., T. Karl, P. Harley, C. Wiedinmyer, P. I. Palmer, and C. Geron, 2006: Estimates of global terrestrial isoprene emissions using MEGAN (Model of Emissions of Gases and Aerosols from Nature). *Atmos. Chem. Phys.*, **6**, 3181–3210.
- Hallquist, M., and Coauthors, 2009: The formation, properties and impact of secondary organic aerosol: Current and emerging issues. *Atmos. Chem. Phys.*, **9**, 5155–5236, doi:10.5194/acp-9-5155-2009.
- Hansel, A., A. Jordan, R. Holzinger, P. Prazeller, W. Vogel, and W. Lindinger, 1995: Proton transfer reaction mass spectrometry: On-line trace gas analysis at the ppb level. *Intl. J. Mass Spectrom.*, **149–150**, 609–619.
- Harman, I. N., and J. J. Finnigan, 2008: Scalar concentration profiles in the canopy and roughness sublayer. *Bound.-Layer Meteorol.*, **129**, 323–351, doi:10.1007/s10546-008-9328-4.
- Haverd, V., M. Cuntz, R. Leuning, and H. Keith, 2007: Air and biomass heat storage fluxes in a forest canopy: Calculation within a soil vegetation atmosphere transfer model. *Agric. For. Meteorol.*, **147**, 125–139.
- Held, A., E. Patton, L. Rizzo, J. Smith, A. Turnipseed, and A. Guenther, 2008: Relaxed eddy accumulation simulations of aerosol number fluxes and potential proxy scalars. *Bound.-Layer Meteorol.*, **129**, 451–468, doi:10.1007/s10546-008-9327-5.
- Horst, T. W., J. Kleissl, D. H. Lenschow, C. Meneveau, C.-H. Moeng, M. B. Parlange, P. P. Sullivan, and J. C. Weil, 2004: HATS: Field observations to obtain spatially filtered turbulence fields from crosswind arrays of sonic anemometers in the atmospheric surface layer. *J. Atmos. Sci.*, **61**, 1566–1581.
- Karl, T., A. Guenther, A. Jordan, R. Fall, and W. Lindinger, 2000: Covariance measurements of biogenic oxygenated VOC emissions from hay harvesting. *Atmos. Environ.*, **35**, 491–495.
- , C. Spirig, J. Rinne, C. Stroud, P. Prevost, J. Greenberg, R. Fall, and A. Guenther, 2002: Virtual disjunct eddy covariance measurements of organic compound fluxes from a subalpine forest using proton transfer reaction mass spectrometry. *Atmos. Chem. Phys.*, **2**, 279–291.
- , A. Guenther, A. Turnipseed, E. Patton, and K. Jardine, 2008: Chemical sensing of plant stress at the ecosystem scale. *Biogeosciences*, **5**, 1287–1294.
- Kurpius, M., and A. H. Goldstein, 2003: Gas-phase chemistry dominates O<sub>3</sub> loss to a forest, implying a source of aerosols and hydroxyl radicals to the atmosphere. *Geophys. Res. Lett.*, **30**, 1371, doi:10.1029/2002GL016785.
- Lee, A., G. W. Schade, R. Holzinger, and A. H. Goldstein, 2005: A comparison of new measurements of total monoterpene flux with improved measurements of speciated monoterpene flux. *Atmos. Chem. Phys.*, **5**, 505–513.
- Leff, J. W., and N. Fierer, 2008: Volatile organic compound (VOC) emissions from soil and litter samples. *Soil Biol. Biochem.*, **40**, 1629–1636.
- Lenschow, D. H., J. Mann, and L. Kristensen, 1994: How long is long enough when measuring fluxes and other turbulent statistics? *J. Atmos. Oceanic Technol.*, **11**, 661–673.
- Lindinger, W., A. Hansel, and A. Jordan, 1998: Proton-transfer-reaction mass spectrometry (PTR-MS): On-line monitoring of volatile organic compounds at pptv levels. *Chem. Soc. Rev.*, **27**, 347–375.
- Mayor, S. D., 2011: Observations of seven atmospheric density current fronts in Dixon, California. *Mon. Wea. Rev.*, in press.

- , and E. W. Eloranta, 2001: Two-dimensional vector wind fields from volume imaging lidar data. *J. Appl. Meteor.*, **40**, 1331–1346.
- , and S. M. Spuler, 2004: Raman-shifted eye-safe aerosol lidar. *Appl. Opt.*, **43**, 3915–3924.
- , —, B. M. Morley, and E. Loew, 2007: Polarization lidar at 1.54 microns and observations of plumes from aerosol generators. *Opt. Eng.*, **46**, 096201, doi:10.1117/12.781902.
- Mikkelsen, T. N., H. Ro-Poulsen, K. Pilegaard, M. F. Hovmand, N. O. Jensen, C. S. Christensen, and P. Hummelshøj, 2000: Ozone uptake by an evergreen forest canopy: Temporal variation and possible mechanisms. *Environ. Pollut.*, **109**, 423–429.
- Nishiyama, R. T., and A. J. Bedard Jr., 1991: A “quad-disk” static pressure probe for measurement in adverse atmospheres—With a comparative review of static pressure probe designs. *Rev. Sci. Instrum.*, **62**, 2193–2204.
- Patton, E. G., J. C. Weil, and P. P. Sullivan, 2008: A coupled canopy-soil model for the simulation of the modification of atmospheric turbulence by tall vegetation. *Extended Abstracts, 18th Symp. on Boundary Layers and Turbulence*, Stockholm, Sweden, Amer. Meteor. Soc., 9A.3. [Available online at [http://ams.confex.com/ams/18BLT/techprogram/paper\\_140168.htm](http://ams.confex.com/ams/18BLT/techprogram/paper_140168.htm).]
- Pope, S. B., 2000: *Turbulent Flows*. Cambridge University Press, 771 pp.
- Rannik, U., M. Aubinet, O. Kurbanmuradov, K. K. Sabelfeld, T. Markkanen, and T. Vesala, 2000: Footprint analysis for measurements over a heterogeneous forest. *Bound.-Layer Meteor.*, **97**, 137–166, doi:10.1023/A:1002702810929.
- Raupach, M. R., J. J. Finnigan, and Y. Brunet, 1996: Coherent eddies and turbulence in vegetation canopies: The mixing-layer analogy. *Bound.-Layer Meteor.*, **78**, 351–382.
- Rinne, H. J. I., A. B. Guenther, C. Warneke, J. A. de Gouw, and S. L. Luxembourg, 2001: Disjunct eddy covariance technique for trace gas flux measurements. *Geophys. Res. Lett.*, **28**, 3139–3142.
- Ryan, M. G., and B. Law, 2005: Interpreting, measuring, and modeling soil respiration. *Biogeochemistry*, **73**, 3–27.
- Shaw, R. H., and U. Schumann, 1992: Large-eddy simulation of turbulent flow above and within a forest. *Bound.-Layer Meteor.*, **61**, 47–64, doi:10.1007/BF02033994.
- , and E. G. Patton, 2003: Canopy element influences on resolved- and subgrid-scale energy within a large-eddy simulation. *Agric. For. Meteor.*, **115**, 5–17.
- Shulaev, V., P. Silverman, and I. Raskin, 1997: Airborne signalling by methyl salicylate in plant pathogen resistance. *Nature*, **385**, 718–721.
- Spirig, C., and Coauthors, 2005: Eddy covariance flux measurements of biogenic VOCs during ECHO 2003 using proton transfer reaction mass spectrometry. *Atmos. Chem. Phys.*, **5**, 465–481.
- Spuler, S. M., and S. D. Mayor, 2005: Scanning eye-safe elastic backscatter lidar at 1.54  $\mu\text{m}$ . *J. Atmos. Oceanic Technol.*, **22**, 696–703.
- Sullivan, P. P., T. W. Horst, D. H. Lenschow, C.-H. Moeng, and J. C. Weil, 2003: Structure of subfilter-scale fluxes in the atmospheric surface layer with application to large-eddy simulation modelling. *J. Fluid Mech.*, **482**, 101–139.
- Tong, C., J. C. Wyngaard, S. Khanna, and J. G. Brasseur, 1998: Resolvable- and subgrid-scale measurement in the atmospheric surface layer: Technique and issues. *J. Atmos. Sci.*, **55**, 3114–3126.
- Weil, J. C., P. P. Sullivan, and C.-H. Moeng, 2004: The use of large-eddy simulations in Lagrangian particle dispersion models. *J. Atmos. Sci.*, **61**, 2877–2887.
- Wilczak, J. M., and A. J. Bedard Jr., 2004: A new turbulence microbarometer and its evaluation using the budget of horizontal heat flux. *J. Atmos. Oceanic Technol.*, **21**, 1170–1181.
- Williams, E. J., G. L. Hutchinson, and F. C. Fehsenfeld, 1992:  $\text{NO}_x$  and  $\text{N}_2\text{O}$  emissions from soil. *Global Biogeochem. Cycles*, **6**, 351–388.
- Wyngaard, J. C., 1984: Large-eddy simulation: Guidelines for its application to planetary-boundary layer research. U.S. Army Research Office Tech. Rep. 0804, 122 pp.
- Zhu, W., R. van Hout, and J. Katz, 2007: On the flow structure and turbulence during sweep and ejection events in a wind-tunnel model canopy. *Bound.-Layer Meteor.*, **124**, 205–233, doi:10.1007/s10546-007-9174-9.

# SHOP

the new AMS online bookstore



Use this **easy-to-navigate** site to review and purchase new and classic titles in the collection of AMS Books—including general interest weather books, histories, biographies, and monographs—plus much more.

**View** tables of contents, information about the authors, and independent reviews.

As always, **AMS members receive deep discounts** on all AMS Books.

[www.ametsoc.org/amsbookstore](http://www.ametsoc.org/amsbookstore)

The new AMS online bookstore is now open.

**Booksellers and wholesale distributors** may set up accounts with our distributor, The University of Chicago Press, by contacting Karen Hyzy at [khyzy@press.uchicago.edu](mailto:khyzy@press.uchicago.edu), 773-702-7000, or toll-free at 800-621-2736.

**AMS BOOKS**

RESEARCH APPLICATIONS HISTORY